Proc. Natl. Acad. Sci. USA
Vol. 77, No. 8, pp. 4726–4730, August 1980
Biophysics

Location of the chromophore in bacteriorhodopsin

(purple membrane/neutron diffraction/halobacteria/light energy transduction/proton translocation)

G. I. KING*, P. C. MOWERY*, W. STOECKENIUS*, H. L. CRESPI†, AND B. P. SCHOENBORN‡

*Department of Biochemistry and Biophysics and Cardiovascular Research Institute, University of California, San Francisco, California 94143; †Argonne National Laboratory, Argonne, Illinois 60439; and ‡Department of Biology, Brookhaven National Laboratory, Upton, New York 11973

Contributed by Walther Stoeckenius, May 23, 1980

ABSTRACT **We present a location for the retinylidene chromophore in dark-adapted bacteriorhodopsin based on the differences in neutron scattering between purple membrane preparations reconstituted with retinal and with deuterated retinal. The Fourier difference density map contains more peaks than expected, and additional arguments are introduced to exclude artificial peaks caused by the reconstitution techniques or the limited resolution of the diffraction data. The membrane preparation used is necessarily dark-adapted and therefore contains 13-*cis*- and all-*trans*-retinal isomers in roughly equal amounts. However, we find only a single position for both isomers. Presumably, the difference in conformation caused by isomerization around the C13–C14 double bond is minimized by rotation around other bonds. The retinal is located between α-helical segments of the protein and its nearest neighbor (intratrimer) distance is 26 Å; the next-nearest neighbor (intertrimer) distance is 38 Å.**

The purple membrane occurs as differentiated patches in the cell membrane of halobacteria. It contains only one protein, bacteriorhodopsin (bR), of molecular weight 26,500; the amino acid sequence is known (1, 2). It has a strong absorption band between 500 and 600 nm due to covalently bound retinal. bR converts light energy into an electrochemical proton gradient, which drives energy-requiring metabolic processes such as ATP synthesis and amino acid transport (3–5). The crystalline array of bR in the plane of the purple membrane has made it possible to determine the membrane structure at high resolution. Henderson and Unwin (6), using low-dose electron microscopy, obtained a three-dimensional scattering density map at 7-Å resolution in the plane of the membrane and at 14-Å resolution normal to it. The protein apparently consists of seven α-helical rods, about 40 Å long and 10 Å apart, all oriented roughly perpendicular to the membrane plane and arranged in two parallel rows. This model has been confirmed by Hayward *et al.* (7). The lipids occupy the interstices of the protein lattice in a bilayer orientation (8).

The group of α-helical segments shown below in Fig. 2 is thought to represent one molecule of bR; this has recently been confirmed by low-dose electron microscopy of a different crystalline form of purple membrane (9). The three molecules clustered around the 3-fold axis at the origin of the unit cell are usually referred to as the trimer. Retinal is bound as a protonated Schiff base to the ε-amino group of lysine-41 (1, 2, 10, 11). bR exists in two interconvertible forms, light-adapted and dark-adapted, characterized by differences in their absorption maxima and extinction coefficients. Extraction of the chromophore from the light-adapted form yields primarily all-*trans*-retinal. The dark-adapted form yields an equimolar ratio of 13-*cis*- and all-*trans*-retinal (12, 13). Although resonance Raman spectra indicate that the retinal conformations in the membrane may not correspond exactly to those of 13-*cis* isomers in solution (14–16), we shall refer to the conformers *in situ* as 13-*cis* and all-*trans* because these are the best available approximations.

Resonance Raman spectra of bR and its photocycle intermediates (17) strongly suggest that the retinylidene Schiff base is directly involved in proton transport across the membrane. This has led us to examine the location of retinal in the membrane. The retinylidene imine can be exchanged if the chromophore is bleached with hydroxylamine under intense illumination, followed by regeneration with added 13-*cis*- or all-*trans*-retinal (18, 19). In this paper, we report the position of the retinylidene isomers in the membrane plane as determined by a neutron-scattering Fourier difference density map between samples regenerated with normal and with deuterated retinal, respectively. We have reported previously that the β-ionone ring of the molecule is located near the center of the membrane profile (20).

MATERIALS AND METHODS

Preparation of Deuterated Membrane. Fully deuterated purple membrane was obtained from *Halobacterium halobium* R_1 which was grown in a nutrient medium consisting of heavy water (^2H_2O) containing 99.7 atom percent ^2H, salts, and 20 ml of the granular syrup obtained from acid hydrolysis of fully deuterated algae per liter (21, 22). The culture conditions have been described (20). Both ^2H-containing and ^1H-containing purple membranes were prepared by differential centrifugation of cells lysed in distilled water (23). A molar extinction coefficient of $\epsilon_{570} = 63{,}000\ l^{-1}\ mol^{-1}\ cm^{-1}$ for bacteriorhodopsin was used in all calculations.

Purification of Perdeuterated Retinal. All operations were conducted at 0°C under dim red light. All solvents were spectroscopic grade and found to be free of peroxides; they were purged with nitrogen prior to use. Ether was purified by distillation over sodium metal. Fully deuterated purple membrane was lipid-extracted by the method of Bligh and Dyer (24). The nonpolar lipids were dissolved in 2% ether/hexane, and perdeuterated 13-*cis*- and all-*trans*-retinals were isolated on a Waters ALC/GPC 204 chromatograph fitted with a dual-wavelength detector (365 and 254 nm) and a μ-Porasil column; the eluent was 2% ether-hexane (13). The purity of the retinal isomers was checked by chromatography and by UV spectra.

Reconstitution of Bacteriorhodopsin. Apomembrane was prepared by photobleaching with 1.0 M NH_2OH/10 mM HEPES, pH 7.0, as described by Bauer *et al.* (25) and was reconstituted as described by Oesterhelt and Schuhmann (19), with a mixture of 13-*cis* and all-*trans* isomers of either hydrogen-containing retinal ($R\text{-}H_{28}$) or perdeuterated retinal ($R\text{-}^2H_{28}$) in stoichiometric amounts. This reconstitutes 84% of the original band of absorbance at 570 nm.

The publication costs of this article were defrayed in part by page charge payment. This article must therefore be hereby marked "*advertisement*" in accordance with 18 U. S. C. §1734 solely to indicate this fact.

Abbreviation: bR, bacteriorhodopsin.

Extraction of Retinal Oxime. The bleaching technique leaves retinal oxime bound to the membrane. To remove it, we adapted the method for extracting ubiquinone from submitochondrial particles, as developed by Szarkowska (26) and modified by Ernster *et al.* (27), using anhydrous hexane instead of pentane. All work was done in a cold room. Reconstituted purple membrane (at most, 0.62 μmol of bR per tube) was freeze-dried overnight, extracted with six 5-ml aliquots of hexane (dried over $CaSO_4$), and spun down in a bench top centrifuge. The residual hexane was removed under reduced pressure, and the samples were resuspended in water prior to use.

Spectral Studies. Purple membrane films with an absorbance of 0.6 were prepared by drying purple membrane suspensions on cover glasses at ambient humidity as described by Heyn *et al.* (28). The films were mounted at an angle of 45° to the incident beam. Spectra were scanned between 750 and 450 nm with a Polaroid sheet in the parallel and perpendicular orientations and stored in a Nicolet 1180 computer, and the dichroic ratios were calculated. The angle θ of the chromophore relative to the membrane plane was calculated as described by Heyn *et al.* (28), with 570-nm light, a refractive index of 1.5, and a mosaic spread of 7°. In addition, the angle θ for the retinal oxime was measured at 366 nm. Three films of each membrane sample were used.

Neutron Diffraction Experiments. Two samples of purple membrane regenerated with R-H_{28} and R-$^2H_{28}$ were suspended in H_2O and placed on thin aluminum sheets. Excess water was allowed to evaporate until the membrane formed stacks of hydrated, approximately parallel layers. The aluminum sheets were then formed into a sandwich with aluminum spacers and placed in a container at a constant relative humidity of 100%; the temperature was controlled between 10 and 15°C to avoid condensation on the sample. About 150 mg of membrane was used for each sample.

Neutron diffraction data were collected at the high-flux beam reactor at Brookhaven National Laboratory on a paired Soller slit, step-scanning diffractometer. Soller slit collimators were placed before and after the specimen. A graphite monochromator was used to select a wavelength band at 4.2 Å from the scattered neutrons, which was Bragg reflected into a ^3He detector. Some neutron diffraction experiments were also performed by using a two-dimensional position-sensitive detector. The details of the experimental arrangement, as well as the data reduction scheme, have been described (20). The Soller slit arrangement gave superior results and the analysis reported here will be confined to those data. The samples were oriented in the camera with the plane of the membrane sheets normal to the neutron beam. The in-plane diffraction from this geometry presents essentially a two-dimensional powder pattern because the membranes are randomly oriented in the layer plane. Diffraction intensities were collected out to a resolution of 8.7 Å (Fig. 1).

RESULTS AND DISCUSSION

In order to minimize the differences between the deuterated and nondeuterated samples due to bleaching and reconstitution, each sample of purple membrane was bleached and divided in half, and the halves were reconstituted with equivalent molar quantities of R-H_{28} and R-$^2H_{28}$, respectively. However, the bleaching process produces 1 mol of retinal oxime per mol of bR, which remains bound to the membrane and might cause problems. Residual hydroxylamine may react directly with the added retinal, producing deuterated retinal oxime which will be bound by the membrane. An exchange of the oxime with the imine function of the added deuterated retinal could also produce deuterated oxime as a contaminant. We therefore extracted as much of the oxime as possible without destroying the purple membrane structure. Samples of apomembrane and reconstituted purple membrane were lyophilized and extracted with hexane. The bleached membrane was then reconstituted, and the absorption, linear dichroism, and circular dichroism spectra, the light-dark adaptation, and the x-ray diffraction patterns of the samples were compared. More than 80% of the oxime was removed from bleached membrane, whereas only 50–60% was extracted from reconstituted membrane. The chromophore apparently protects the structure of the purple membrane. When the apomembrane was extracted, all measured properties were adversely affected (Tables 1 and 2). Furthermore, the extracted apomembrane aggregated both before and after reconstitution. We therefore used only membranes extracted after reconstitution in the initial neutron

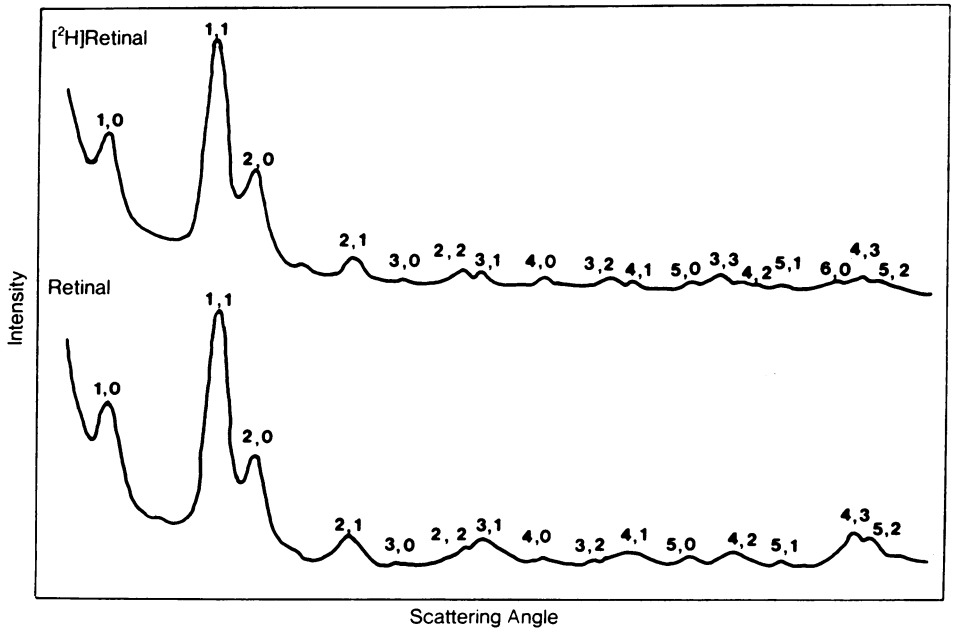

FIG. 1. Neutron diffraction intensities from purple membrane with retinal-H_{28} and with retinal-$^2H_{28}$.

Table 1. Effect of retinal oxime extraction on reconstitution

Preparation	% oxime extracted*	λ_{max}, nm Light	Dark	Width at half-height,† cm^{-1}	Dark adaptation, % ΔA	Exciton splitting	Lattice, x-ray
Purple membrane (native)	—	570	560	3100	13	Yes	Yes
Reconstituted	—	570	560	3300	10.5	Yes	Yes
Extracted, reconstituted	>80	570	565	5100	−3.7‡	Yes	No
Reconstituted, extracted	50–60	570	560	3400	9.5	Yes	Yes

* Calculated from the ratio A_{570}/A_{360} before and after extraction.
† Light-adapted pigments.
‡ Relative absorbance reversed (bleaching).

diffraction experiments. The small sample sizes in these experiments (≈20 mg) required use of the two-dimensional detector. Preliminary analysis showed that the presence of the oxime did not seriously affect the data. In order to minimize sample loss, we omitted the extraction step for the larger samples needed in the Soller slit experiments.

For a complete structural analysis based on the differences in neutron scattering between the two isotopically different samples, we used sets of structure factors for each and the set of phase angles for the "native" structure. The sets of intensities, corrected by a Lorentz factor of $(h^2 + hK + K^2)$, provide values for the proper squared structure factors. The phase angle used for each reflection was obtained from Unwin and Henderson's (29) electron microscopic data. Using the electron diffraction phase should be approximately valid because the relative neutron scattering densities (in 20% ^2H_2O) for protein and lipids are similar to the relative electron density values (30). However, a better approximation can be obtained by converting the electron-scattering density map to a neutron-scattering density map with the use of reasonable average conversion factors for bR and purple membrane lipids. The calculated neutron intensities from such a model agree better with the observed neutron diffraction intensities from the R-H_{28} sample than do the electron diffraction data. We therefore consider the phases from the model to be a slightly better choice.

In the diffraction pattern from purple membrane, it is necessary to separate superimposed intensities in some of the observed reflections. We have assumed that the ratios $I_{hk}/(I_{hk} + I_{kh})$ for the neutron intensities (or difference intensities) is the same as in the electron diffraction data of Unwin and Henderson (29). This certainly is only an approximation. However, we have calculated the Fourier map for the sample reconstituted with R-H_{28} (Fig. 2), using the neutron amplitudes and phases calculated from Unwin and Henderson's model, as indicated in the preceding paragraph. The resulting map is similar to the electron-scattering density map (29), indicating that this treatment of superimposed reflections may be acceptable. To calculate a Fourier difference map, it is necessary to obtain sets of properly scaled structure factors from the normal and deuterated retinal samples; we used the scaling procedure of Kraut *et al.* (31) for this purpose.§ The difference map (Fig. 3) was calculated from the difference in scaled amplitudes between the two data sets with the same phase angles as for the map in Fig. 2. The position(s) of the retinylidene moieties projected onto the membrane plane should appear as density peaks in the map. The map shows a prominent peak, labeled 1, connected to a slightly less prominent peak, labeled 2, and numerous other less pronounced peaks.

Before trying to interpret the difference Fourier map, we should point out that the samples used for membrane diffraction have an extremely high optical density, ≈50 absorbance units, and that, during the exposure time, 24 hr, necessary to collect sufficient diffracted intensities, the samples are in the dark. Even though no special precautions were taken to prevent light exposure during preparation, the membranes should therefore be in the dark-adapted state—i.e., they should contain approximately equal amounts of 13-*cis* and all-*trans* isomers (12, 13). Our linear dichroism measurements on oriented multilayers of light-adapted purple membrane show that the

Table 2. Linear dichroism of purple membrane films

Sample	θ at 570 nm	θ at 366 nm
Purple membrane	25.6 ± 1.1	—
Apomembrane	—	31.1 ± 0.6
Reconstituted membrane	22.0 ± 1.3	47.3 ± 1.0
Reconstituted, extracted	22.0 ± 0.8	54.3 ± 1.3

The data for each sample represent the mean ± SD from the analysis of three films. The absolute error is estimated to be ±5%, which includes uncertainties in the index of refraction of the absorption bands in the films.

§ The scaling expression as published in their paper is incorrect; the multiplicative factor of ½ in their expression should be 2.

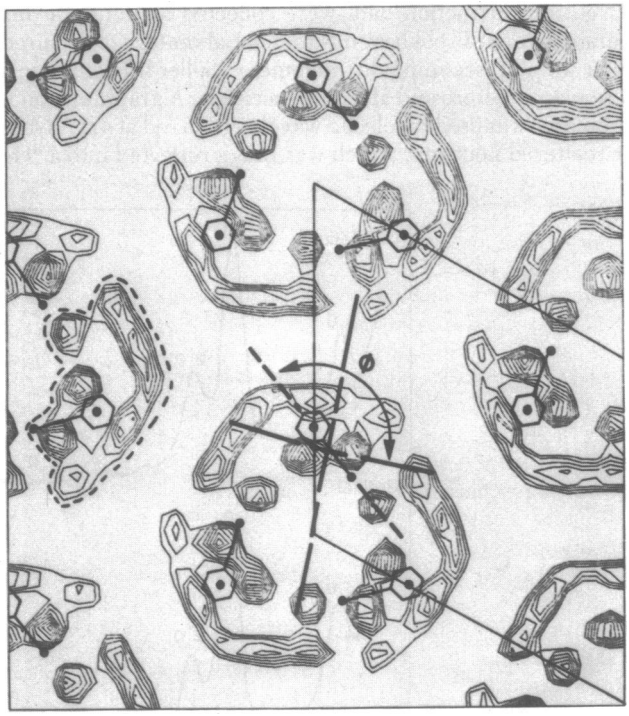

FIG. 2. Fourier synthesis map of dark-adapted purple membrane calculated from the neutron intensities of the retinal-H_{28} sample and the phases obtained from electron microscopy. The unit cell is outlined, and the α-helical segments assumed to belong to one molecule of bR are enclosed by a dashed line. Positions for the retinal molecules are indicated (⊙—•). Negative contour lines have been omitted.

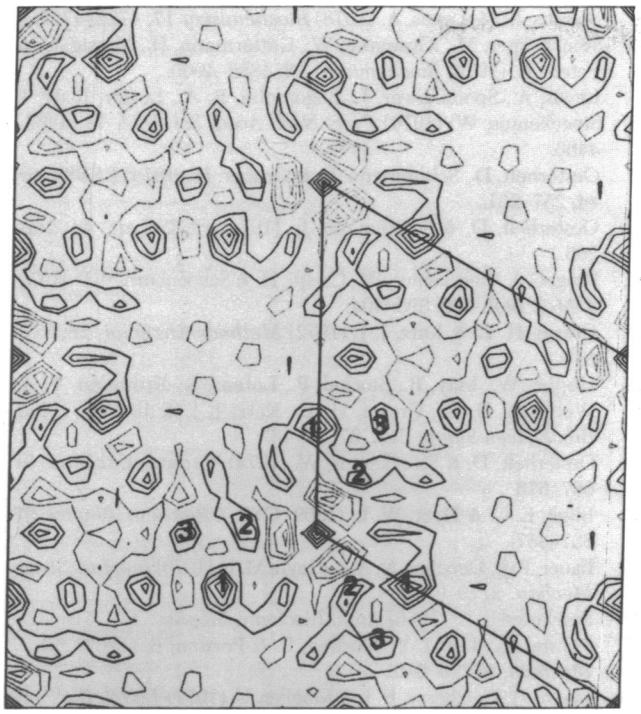

FIG. 3. Difference Fourier synthesis map between intensities from retinal-H_{28} and retinal-$^2H_{28}$ samples with the same phases as in Fig. 1.

transition moment of the chromophore, and therefore its long axis, is oriented at an angle of ±23° with respect to the membrane plane (Table 2; refs. 28 and 32) and that this angle changes little during dark-adaptation (32). There is also no detectable change of the in-plane orientation (ref. 33; unpublished results). The difference in spatial requirements for the two isomers apparently is minimized by simultaneous rotations about other bonds in the lysine or along the retinylidenelysine backbone. This conclusion is further borne out by the absence of significant differences in the x-ray diffraction patterns from light- and dark-adapted membrane (unpublished data). At our limited resolution, we therefore expect to observe only one position for the chromophore.

Taking the distribution of hydrogens in retinal into account, the projection of one retinylidene moiety onto the plane of the membrane should show a high-density region corresponding to the deuterated β-ionone ring and a relatively uniform density, about one-third that of the ring, corresponding to the deuterated hydrocarbon chain. At an out-of-plane angle of 23°, the projected length of the molecule is about 14 Å. The projected density distribution, at our resolution of 8.7 Å, should then consist of one peak representing the β-ionone ring position connected to another smaller peak, about 12 Å away, representing the Schiff base region, which should also appear as a peak due to the series termination error. We then identify peak 1 in Fig. 3 as the β-ionone ring of the retinal because it is the most prominent peak in the map, and peak 2 as the Schiff base end of the chromophore. This assignment is further justified by model calculations, which we will discuss next.

In addition to the features described above, Fig. 3 also contains other peaks of lesser density. It is not difficult to show that these peaks can be attributed to series termination errors—i.e., that they are due to the low resolution (8.7 Å) of the maps. A model map was calculated from the difference structure factors between the native map described previously and the same map with a deuterated retinal added to it in the location of peaks 1 and 2 as described above. This model difference map (Fig. 4) is similar to the one in Fig. 3. Model difference Fourier maps (not shown) corresponding to other possible interpretations of the observed map—for instance, assuming peak 2 to be the Schiff base and peak 1 or 3 to be the β-ionone ring position—do not agree with Fig. 3 as closely. However, model maps for one alternative arrangement give an agreement only slightly worse than that for our preferred position: peak 1 could represent the β-ionone ring and peak 3, the Schiff base. Further experiments with a retinal only deuterated near the Schiff base should resolve this issue conclusively.

The structural data reported here are in conflict with a chromophore geometry calculated from spectral data. Ebrey *et al.* (34), using exciton theory, assumed that intertrimer interactions were negligible and obtained a reasonable fit between observed and calculated spectra with an interchromophore distance r of 15 Å, an angle θ between the transition dipole and the membrane plane of 19°, and an angle ϕ (cf. Fig. 2) of 85°. Our data yield $\theta = 25°$, $\phi = 135°$, and $r = 26$ Å. Our nearest-neighbor distance between the retinylidene moieties agrees well with earlier estimates from our laboratory, which were based on linear and circular dichroism measurements (35). Furthermore, the intertrimer chromophore distance is 38 Å. Because dipolar chromophore interactions vary with r^{-3}, intratrimer effects are only 3 times more favorable than intertrimer effects. Clearly, the spectral data should be reevaluated on the basis of the experimental chromophore geometry.

Our data define the orientation of retinal and the position of its Schiff base if we accept Bridgen and Walker's (11) identification of lysine-41 as the retinal-binding residue. Therefore, the α-helical segment under peak 2 should be the second α-helical segment, counting from the amino terminus of the polypeptide chain. If the location of connections between α-helical segments can now be determined, which may be possible from existing data (unpublished results), the amino acid sequence can be coordinated with the scattering density map. This should yield important information about the protein

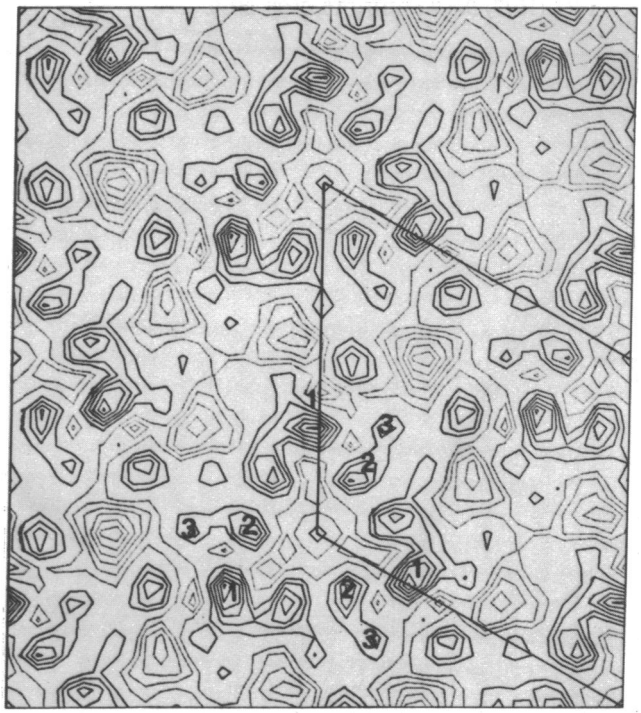

FIG. 4. Model difference Fourier synthesis map between calculated intensities from retinal-H_{28} and retinal-$^2H_{28}$ models (see text for explanation).

environment of the retinal, which is essential for further elucidation of its function.

We thank Dr. Richard Henderson for supplying us with the electron diffraction phase angles and amplitudes used in our analysis. Special thanks are also given to Drs. Robert Stroud and David Agard for many useful discussions as well as the use of their computer facilities for the contour plots. We also acknowledge the advice and help of Dr. Roberto Bogomolni. This work was supported by grants from the National Institutes of Health (Program Project HL-06285) and the National Aeronautics and Space Administration (NSG-07151). The deuterated bacteria were grown at Argonne National Laboratory under the auspices of the Office of Basic Energy Sciences of the Department of Energy. Neutron scattering data were collected under the auspices of the Department of Energy.

1. Ovchinnikov, Y. A., Abdulaev, N. G., Feigina, Y. M., Kiselev, A. V. & Lobanov, N. A. (1979) *FEBS Lett.* **100,** 219–224.
2. Khorana, H. G., Gerber, G. E., Herlihy, W. C., Gray, C. P., Anderegg, R. J., Nihei, K. & Biemann, K. (1979) *Proc. Natl. Acad. Sci. USA* **76,** 5046–5050.
3. Oesterhelt, D. & Stoeckenius, W. (1973) *Proc. Natl. Acad. Sci. USA* **70,** 2853–2857.
4. Danon, A. & Stoeckenius, W. (1974) *Proc. Natl. Acad. Sci. USA* **71,** 1234–1238.
5. MacDonald, R. E. & Lanyi, J. K. (1977) *Fed. Proc. Fed. Am. Soc. Exp. Biol.* **36,** 1828–1832.
6. Henderson, R. & Unwin, P. N. T. (1975) *Nature (London)* **257,** 28–32.
7. Hayward, S. B., Grano, D. A., Glaeser, R. M. & Fisher, K. A. (1978) *Proc. Natl. Acad. Sci. USA* **75,** 4320–4324.
8. Blaurock, A. E. & King, G. I. (1977) *Science* **196,** 1101–1104.
9. Michel, H., Oesterhelt, D. & Henderson, R. (1980) *Proc. Natl. Acad. Sci. USA* **77,** 338–342.
10. Oesterhelt, D. & Stoeckenius, W. (1971) *Nature (London) New Biol.* **233,** 149–152.
11. Bridgen, J. & Walker, I. D. (1976) *Biochemistry* **15,** 792–798.
12. Oesterhelt, D., Meentzen, M. & Schumann, L. (1973) *Eur. J. Biochem.* **40,** 453–463.
13. Pettei, M., Yudd, A. P., Nakanishi, K., Henselman, R. & Stoeckenius, W. (1977) *Biochemistry* **16,** 1955–1958.
14. Aton, B., Doukas, A. G., Callender, R. H., Becher, B. & Ebrey, T. G. (1977) *Biochemistry* **16,** 2995–2999.
15. Marcus, M. & Lewis, A. (1978) *Biochemistry* **17,** 4722–4728.
16. Stockburger, M., Klusmann, W., Gattermann, H., Massig, G. & Peters, R. (1979) *Biochemistry* **18,** 4886–4900.
17. Lewis, A., Spoonhower, J., Bogomolni, R. A., Lozier, R. H. & Stoeckenius, W. (1974) *Proc. Natl. Acad. Sci. USA* **71,** 4462–4466.
18. Oesterhelt, D., Schuhmann, L. & Gruber, H. (1974) *FEBS Lett.* **44,** 257–261.
19. Oesterhelt, D. & Schuhmann, L. (1974) *FEBS Lett.* **44,** 262–265.
20. King, G. I., Stoeckenius, W., Crespi, H. & Schoenborn, B. P. (1979) *J. Mol. Biol.* **130,** 395–404.
21. Crespi, H. L. & Katz, J. J. (1972) *Methods Enzymol.* **26,** 627–637.
22. Hoppe, W., May, R., Stockel, P., Lorenz, S., Erdmann, V. A., Wettman, H. G., Crespi, H. L., Katz, J. J. & Ibel, K. (1975) *Brookhaven Symp. Biol.* **27,** 38–48.
23. Oesterhelt, D. & Stoeckenius, W. (1974) *Methods Enzymol.* **31,** 667–678.
24. Bligh, E. G. & Dyer, W. L. (1959) *Can. J. Biochem. Physiol.* **37,** 337–357.
25. Bauer, P. J., Dencher, N. A. & Heyn, M. P. (1976) *Biophys. Struct. Mechan.* **2,** 79–92.
26. Szarkowska, L. (1966) *Arch. Biochem. Biophys.* **113,** 519–525.
27. Ernster, L., Lee, I. Y., Norling, B. & Persson, B. (1969) *Eur. J. Biochem.* **9,** 299–310.
28. Heyn, M. P., Cherry, R. J. & Mueller, U. (1977) *J. Mol. Biol.* **117,** 607–620.
29. Unwin, P. N. T. & Henderson, R. (1975) *J. Mol. Biol.* **94,** 425–440.
30. Saibil, H., Chabre, M. & Worcester, D. L. (1976) *Nature (London)* **262,** 266–270.
31. Kraut, J., Seeker, L. C., High, D. F. & Freer, S. T. (1962) *Proc. Natl. Acad. Sci. USA* **48,** 1417–1424.
32. Bogomolni, R. A., Hwang, S.-B., Tseng, Y.-W., King, G. I. & Stoeckenius, W. (1977) *Biophys. J.* **17,** 98a (abstr.).
33. Korenstein, R. & Hess, B. (1978) *FEBS Lett.* **89,** 15–20.
34. Ebrey, T. G., Becher, B., Mao, B., Kilbride, P. & Honig, B. (1977) *J. Mol. Biol.* **112,** 377–397.
35. Bogomolni, R., Hwang, S.-B., Tseng, Y.-W. & Stoeckenius, W. (1978) *Biophys. J.* **21,** 183a (abstr.).